Dbf4 recruitment by forkhead transcription factors defines an upstream rate-limiting step in determining origin firing timing

Dingqiang Fang[1,#], Armelle Lengronne[2,#], Di Shi[1,#], Romain Forey[2], Magdalena Skrzypczak[3], Krzysztof Ginalski[3], Changhui Yan[4], Xiaoke Wang[1], Qinhong Cao[1], Philippe Pasero[2,*], Huiqiang Lou[1,*]

Supplemental information contains Tables S1-S2 and Figures S1-S4.

Table S1. Strains used in this study

Strain	**Genotype**	**Usage**
W303-1a	*MATa trp1-1 ura3-1 his3-11,15 leu2-3,112 ade2-1 can1-100 RAD5*	WT
DF110	W303 *DBF4-13MYC::TRP1*	Fig. 1B
DF111	W303 *FKH1-3HA::KanMX6*	Fig. 1B
DF112	W303 *DBF4-13MYC::TRP1 FKH1-3HA::KanMX6*	Fig. 1B
DF136	W303 *ORC2-3HA::KanMX6 fkh1Δ::NatMX*	Fig. 1E
DF138	W303 *MCM2-3HA::HIS3 fkh1Δ::NatMX*	Fig. 1E
DF201	W303 *6HA-DBF4*	Fig. 1D
DF202	W303 *6HA-DBF4 fkh1Δ::NatMX*	Fig. 1D
DF203	W303 *6HA-DBF4 fkh1Δ::NatMX fkh2ΔC::HIS3*	Fig. 1D
DF172	W303 *SLD3-13MYC::HIS3*	Fig. 5C
DF173	W303 *SLD3-13MYC::HIS3 fkh1Δ::NatMX*	Fig. 5C
DF174	W303 *SLD3-13MYC::HIS3 fkh1Δ::NatMX fkh2ΔC::HIS3*	Fig. 5C, 2F
DF185	W303 *DBF4-5FLAG::KanMX6*	Fig. 1C
DF186	W303 *FKH1-13MYC::HIS3*	Fig. 1C, 2B
DF187	W303 *KanMX6::DBF4-5FLAG HIS3::FKH1-13MYC*	Fig. 1C, 2B
DF301	W303 *dbf4ΔC(656-704)::LEU2*	Fig. 2F, 3C
DF302	W303 *fkh1Δ::NatMX dbf4ΔC(656-704)-forkhead::LEU2*	Fig. 3D
DF304	W303 *dbf4ΔC(656-704)-forkhead::LEU2*	Fig. 3C
DF305	W303 *dbf4ΔC(656-704)-forkhead*::LEU2*	Fig. 3C
DS1	W303 *fkh1Δ::NatMX*	Fig. 2F, 3D, 4
DS6	W303 *fkh1Δ::NatMX DBF4-forkhead::LEU2*	Fig. 4
DS8	W303 *fkh1Δ:: NatMX DBF4-forkhead*::KanMX*	Fig. 4
DS13	W303 *DBF4-GST::KanMX*	Fig. 4

Table S2. Plasmids used in this study

Plasmid	Base plasmid/Genotype	Usage
pET28a-DBF4	kan^r 6His-DBF4	Fig. 1H
pET28a-dbf4C	kan^r 6His-dbf4(656-704)	Fig. 2E
pGEX-4T-1-DBF4	amp^r GST-DBF4	Fig. 5B
pGEX-4T-1-DBF4N	amp^r GST-dbf4(1-390)	Fig. 5B
pGEX-4T-1-FKH1	amp^r GST-FKH1	Fig. 1G, 1H, 2E, 3A
pGEX-4T-1-fkh1(forkhead*)	amp^r GST-fkh1 Δ (NXXRHXXS)	Fig. 3A
pGADT7-FKH1	amp^r/LEU2 GAL4-AD-FKH1	Fig. 1A, 2A, 2D
pGADT7-FKH2	amp^r/LEU2 GAL4-AD-FKH2	Fig. 1A
pGADT7-CDC7	amp^r/LEU2 GAL4-AD-CDC7	Fig. 1A, 2D
pGBKT7-DBF4	kan^r/TRP1 GAL4-BD-DBF4	Fig. 1A, 2A, 5A
pGBKT7-dbf4(67-704)	kan^r/TRP1 GAL4-BD-dbf4(67-704)	Fig. 2D
pGBKT7-dbf4(1-655)	kan^r/TRP1 GAL4-BD-dbf4(1-655)	Fig. 2D
pGBKT7-dbf4(656-704)	kan^r/TRP1 GAL4-BD-dbf4(656-704)	Fig. 2D
pGBKT7-dbf4(1-680)	kan^r/TRP1 GAL4-BD-dbf4(1-680)	Fig. 2D
pGBKT7-SLD3	kan^r/TRP1 GAL4-BD-SLD3	Fig. 1A, 5A
pGBKT7-SLD7	kan^r/TRP1 GAL4-BD-SLD7	Fig. 1A
pGBKT7-CDC45	kan^r/TRP1 GAL4-BD-CDC45	Fig. 1A, 5A
pGADT7-SLD3	amp^r/LEU2 GAL4-AD-SLD3	Fig. 1A
pGADT7-fkh1-R80A	amp^r/LEU2 GAL4-AD- fkh1-R80A	Fig. 2A
pGADT7-fkh1N	amp^r/LEU2 GAL4-AD- fkh1N	Fig. 2A
pGADT7-fkh1N-R80A	amp^r/LEU2 GAL4-AD- fkh1N-R80A	Fig. 2A
pGADT7-fkh1N-R80A	amp^r/LEU2 GAL4-AD- fkh1N-R80A	Fig. 2A
pGADT7-fkh1C	amp^r/LEU2 GAL4-AD- fkh1C	Fig. 2A
pET28a-SLD3	kan^r 6His-SLD3	Fig. 5B

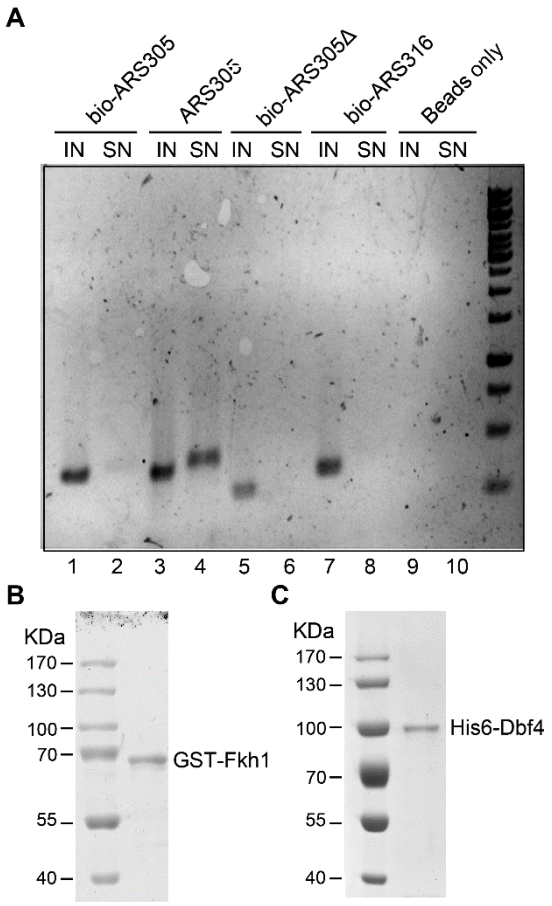

Figure S1

(A) Related to Figure 1F-H. Biotin-labeled *ARS* DNA is efficiently immobilized to the streptavidin beads. Unbound DNA (supernatant, SN) was analyzed by a 2% agarose gel after incubation with the streptavidin beads. The same volume of input DNA (IN) was loaded as a control.

(B, C) Related to Figure 1G-H. SDS-PAGE analysis of purified recombinant proteins Fkh1 (B) and Dbf4 (C). GST-Fkh1 and His6-Dbf4 were expressed and purified following the handbook of the manufacturer.

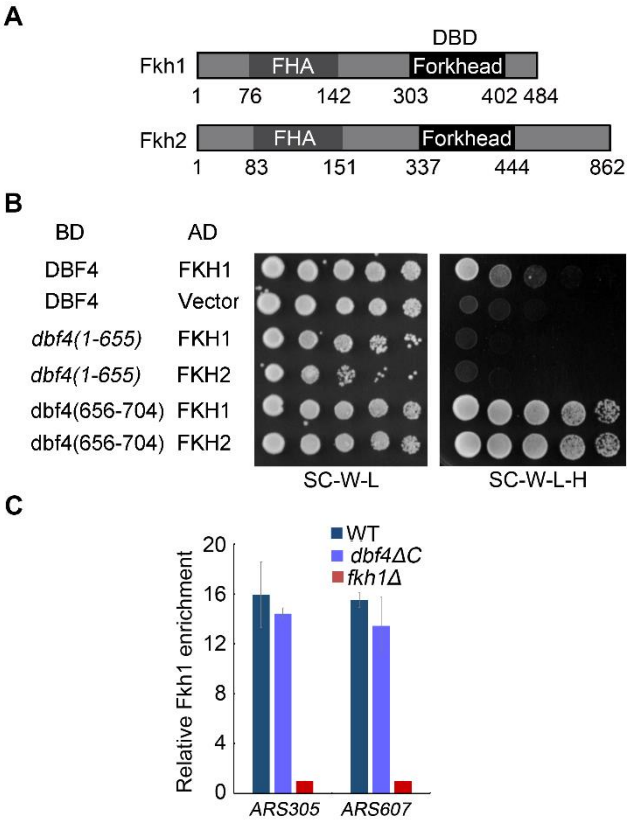

Figure S2- Related to Figure 2.

(A) Domain organizations of Fkh1 and Fkh2. Dark and light grey bars indicate high to moderate sequence identity between them. DBD: DNA binding domain.

(B) C-terminus of Dbf4 mediates interaction with Fkh1/2. Yeast two hybrids were carried out as in Figure 2A. 5-fold serial dilutions of the yeast cells expressing the indicated plasmids were grown at 30℃ on either SC-W-L or SC-W-L-H plates.

(C) Fkh1 persists in binding to early origins in the absence of Dbf4 C-terminus. Fkh1 protein was immunoprecipitated via rabbit multi-clonal antibodies against Fkh1 raised in this study. ChIP assays were conducted basically as described in Figure 1D.

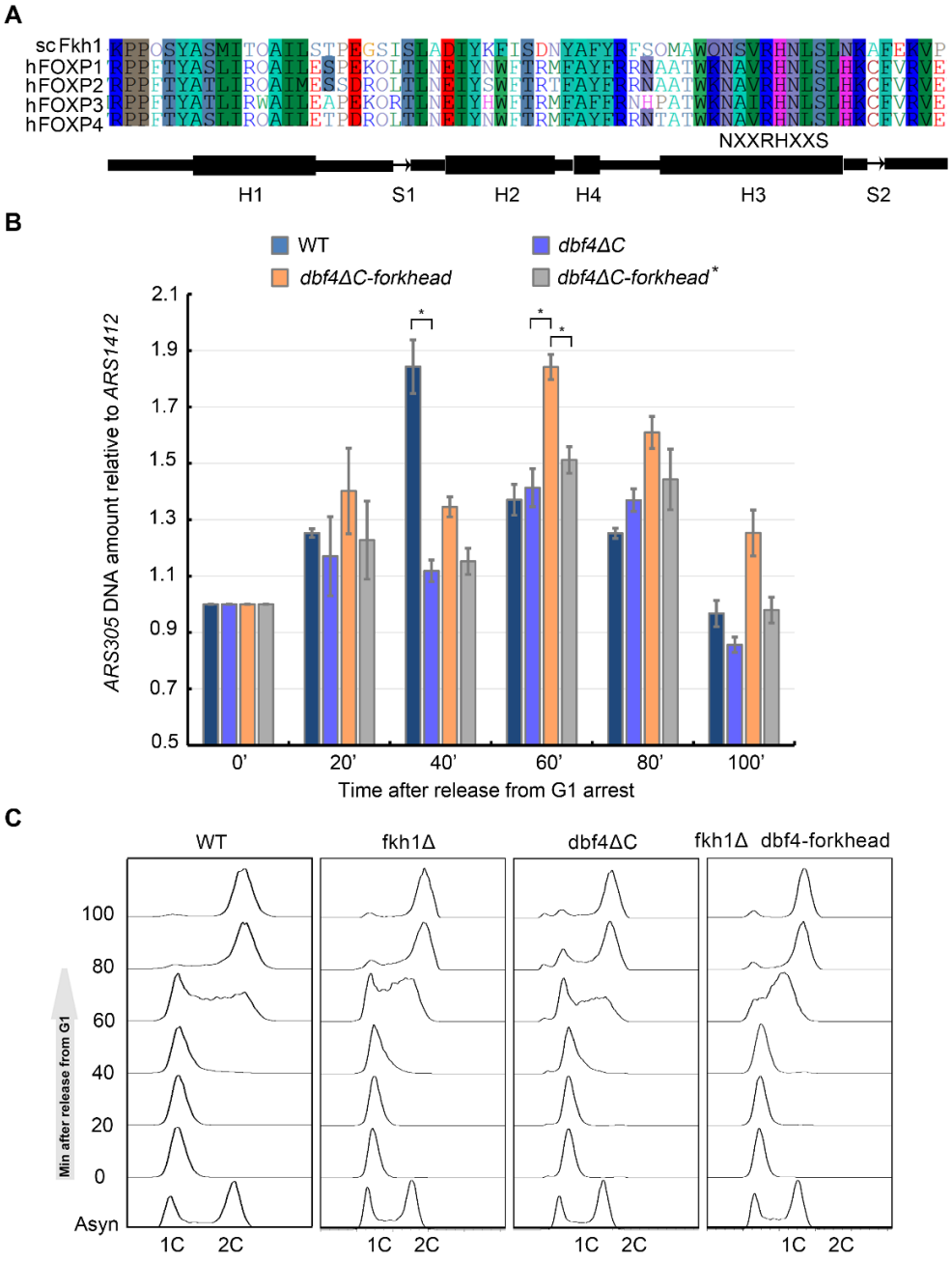

Figure S3- Related to Figure 3.

(A) Amino acid sequence alignment of the forkhead domain of yeast Fkh1 and human forkhead box transcription factors. A conserved motif NxxRHxxS required for DNA binding is indicated.

(B) The deficiency of ARS305 firing can be mostly overcome by fusing Dbf4ΔC with the forkhead domain, but not with the forkhead* mutant. The copy number assays were performed as described in Figure 3C. An average was calculated from three independent experiments; error bars represent SDs. P-value < 0.05 is donated as "*".

(C) Representative flow cytometry profiles of cells used for the copy number assays in Figures 3C and 3D. Cells were synchronized by α-factor and released into fresh media for the indicated time.

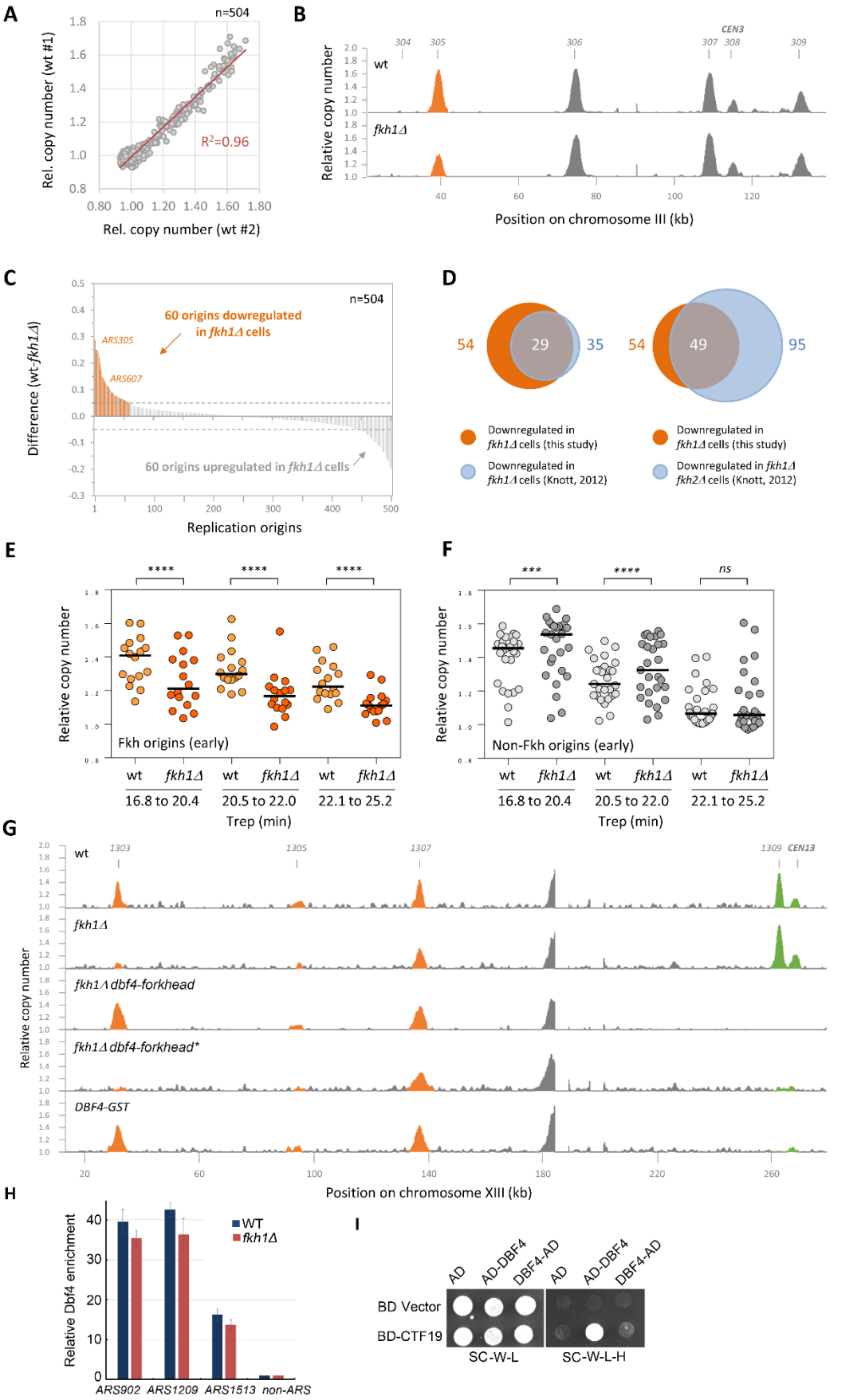
A
n=504
Rel. copy number (wt #1)
Rel. copy number (wt #2)
R²=0.96
B
wt
fkh1Δ
Relative copy number
CEN3
Position on chromosome III (kb)
C
n=504
60 origins dowregulated in fkh1Δ cells
ARS305
ARS607
60 origins upregulated in fkh1Δ cells
Difference (wt-fkh1Δ)
Replication origins
D
54
29
35
54
49
95
Downregulated in fkh1Δ cells (this study)
Downregulated in fkh1Δ cells (Knott, 2012)
Downregulated in fkh1Δ cells (this study)
Downregulated in fkh1Δ fkh2Δ cells (Knott, 2012)
E
Fkh origins (early)
Relative copy number
wt
fkh1Δ
16.8 to 20.4
20.5 to 22.0
22.1 to 25.2
Trep (min)
F
Non-Fkh origins (early)
ns
G
wt
fkh1Δ
fkh1Δ dbf4-forkhead
fkh1Δ dbf4-forkhead*
DBF4-GST
Position on chromosome XIII (kb)
H
Relative Dbf4 enrichment
WT
fkh1Δ
ARS902
ARS1209
ARS1513
non-ARS
I
AD
AD-DBF4
DBF4-AD
BD Vector
BD-CTF19
SC-W-L
SC-W-L-H

Figure S4- Related to Figure 4. Genome-wide analysis of origin usage in WT and in *fkh1Δ* cells

(A) Comparison of the relative copy number around replication origins (n=504) in two biological replicates of WT cells.

(B) Representative region on chromosome III showing the activity of Fkh1-dependent (orange) and Fkh1-independent (grey) origins in WT and *fkh1Δ* cells.

(C) Difference in relative copy number between WT and *fkh1Δ* cells as calculated for 504 annotated origins. 60 origins showing a difference larger than 0.05 (10% of max difference) between WT and *fkh1Δ* cells are labeled in orange.

(D) Venn diagrams of the overlap between 54 origins downregulated in *fkh1Δ* cells (overlap of two biological replicates; this study) and origins downregulated in *fkh1Δ* cells or *fkh1Δ fkh2ΔC* cells (Knott et al. 2012).

(E) Relative copy number at Fkh1-dependent origins in WT and *fkh1Δ* cells, sorted in three groups depending on their time of replication (Trep).

(F) Relative copy number at Fkh1-independent origins in WT and *fkh1Δ* cells, sorted in three groups depending on their time of replication (Trep). ****: $p<0.0001$, *ns*: non-significant, Wilcoxon matched-pairs signed rank test.

(G) Representative regions on chromosome XIII showing the activity of Fkh1-dependent (orange) and *CEN* origins (green) in WT, *fkh1Δ*, *fkh1Δ DBF4-forkhead*, *fkh1Δ DBF4-forkhead** and *DBF4-GST* cells.

(H) Fkh1 does not significantly affect Dbf4 recruitment to *CEN* origins. HA6-Dbf4 was immunoprecipitated via a monoclonal antibody against HA and ChIP was performed as described in Figure 1D.

(I) C-terminal tagging of Dbf4 abolishes the interaction with Ctf19. Yeast two hybrid was basically conducted as described in Figure 1A.

Supplemental References

1. Knott SR, Peace JM, Ostrow AZ, Gan Y, Rex AE, Viggiani CJ, Tavare S, Aparicio OM. Forkhead transcription factors establish origin timing and long-range clustering in *S. cerevisiae*. Cell 2012; 148:99-111.